

STRONG GEOMETRY: KNOTS

BAPTISTE GROS AND JORGE L. RAMÍREZ ALFONSÍN

ABSTRACT. In this paper, we introduce the notion of *strong geometry*, a structure composed by both the chirotope of a set of points X in the d -dimensional space and the *wedge* chirotope which is the specific *adjoint* chirotope induced by the hyperplanes spanned by X . We present various properties relating these two chirotopes, for instance, by introducing the *witness* chirotope, we are able to give a formula expressing the wedge chirotope in terms of the usual chirotope. With this on hand, we answer positively a strong geometry version of a question due to M. Las Vergnas about reconstructing polygonal knots via chirotopes. Moreover, we also show that *linear spatial graphs* are determined by their corresponding strong geometries.

1. INTRODUCTION

Many problems in discrete and convex geometry are based on finite sets of points in the Euclidean space. The combinatorial properties of the underlying point set, rather than its metric properties, are enough to solve a large number of such problems. The codification of the ‘combinatorial properties’ of a point set usually refers to a natural associated notion called *chirotope* (initially known as *combinatorial geometry*, with other equivalent names including *order type* [12] and, in our case, *oriented matroid*). The chirotope captures the relative positions of small tuples of points without taking distances into account [4]. In the affine plane, one such piece of information we can formulate in terms of chirotopes is the intersection properties of the segments spanned by the initial points. However, even though the chirotope tells us which segments intersect, it does not give any information about the relative positions of those intersection (say with respect to the spanned lines). The knowledge of the latter might play a key role in the study of certain geometric problems. For instance, Figure 1 illustrates two hexagons having the same chirotope induced by their vertices (they both have the same set of circuits or equivalently set of minimal Radon partitions). However, in the hexagon on the left the lines joining opposite vertices intersect at point p while they do not on the right one.

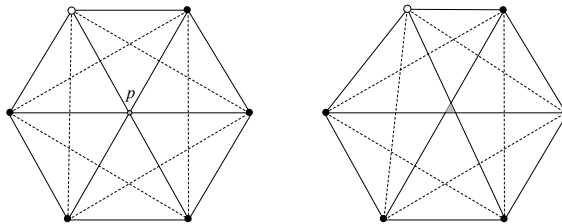


FIGURE 1. (Left) A regular hexagon where point p (in gray) is the intersection of lines joining opposite vertices. (Right) The same regular hexagon in which a vertex (in white) has been slightly moved to the right. The lines joining opposite vertices form a triangle (in gray).

2010 *Mathematics Subject Classification.* 52C140, 57K10.

Key words and phrases. Oriented Matroid, Chirotope, Knot.

It turns out that p is a *0-transversal* to the convex hull of the 4-sets (that is, p intersects all 4-sets formed by the vertices). It can be easily checked that the hexagon on the right does not admit a 0-transversal. In fact, such *discrete transversal* is not necessarily an invariant of the order type, see [6]. This is a typical situation in which the knowledge of the position of the intersection of two lines, with respect with the other spanned lines, is helpful (in this case for a transversality-type problem).

Let X be a vector configuration of $\mathbb{R}^d, d \geq 3$. We introduce the notion of *strong geometry* $S\text{Geom}_{\text{Lin}}(X)$ associated to X . This structure is composed of both the usual linear $M_{\text{Lin}}(X)$ and the *wedge* $M_{\text{Wedge}}(X)$ chirotopes associated to X . The wedge chirotope is a specific *adjoint* chirotope of $M_{\text{Lin}}(X)$ associated to X arising from the spanning vector configuration consisting of exactly one non-zero vector orthogonal to each hyperplane in \mathbb{R}^d that is spanned by a subset of X , see [8, Section 3] (this canonical construction will be treated in detail below). This adjoint lives in the same dimension, but typically it has many more vectors than the original configuration. It is known that every rank 3 oriented matroid has an adjoint [11, 9, 13] but not every oriented matroid has one, for instance, the Vámos matroid has no oriented adjoint [3]. Although a realizable oriented matroid M always admits an adjoint, the latter is not uniquely determined by M , it depends on the particular vector configuration representing M (see below). We refer the reader to [1, 7] and [4, Section 5.3] for further discussions on adjoints for general oriented matroids.

Strong geometries give helpful information, for instance, they encode nicely the combinatorics of the cells of the arrangement of the hyperplanes spanned by a set of points. In Section 6, we discuss different contexts closely connected to strong geometries.

In the Section 3, we treat in detail wedge chirotopes. In rank 3, that is, in the affine plane, we give a formula expressing the wedge chirotope in terms of the usual chirotope for some specific given configuration (see Eq. (3) and Proposition 1). Our approach allows us to get a ‘dimension reduction’ formula for any dimension. More precisely, we show that the chirotope of $M_{\text{Wedge}}(X)$ determines the chirotope of $M_{\text{Aff}}(X)$ up to orientation depending on the parity of the dimension (see Theorem 2 and Corollary 4). In order to show the latter, we introduce the *witness chirotopes* which play a central role for our purpose.

We then focus our attention on the study of a first topological application of strong geometries in connection with geometric knots. A *knot* is an embeddings of S^1 into \mathbb{R}^3 up to ambient isotopy. In order to avoid pathologies, it is common to study tame knots, in particular, *polygonal knots*, that is, closed, piecewise linear loops in \mathbb{R}^3 with no self-intersections. Not much is known about the interplay between the classic setting and *geometric knots*, which are polygonal knots with a fixed number of segments of variable length. Geometric knots are more rigid than smooth knots and are better suited to describe macromolecules (such as DNA) in polymer chemistry and molecular biology, but also far more resistant to investigation.

Let $X = (x_0, \dots, x_{n-1})$ be a n -tuple of points in \mathbb{R}^3 in general position. Let K_X be the polygonal knot defined by the segments $[x_i, x_{i+1}]$ (addition $\pmod n$). Michel Las Vergnas [18] has put forward the following

Question 1. *Let $X = (x_0, \dots, x_{n-1})$ be a n -tuple of points in \mathbb{R}^3 in general position. Is it true that K_X only depends on the chirotope induced by x_0, \dots, x_{n-1} ?*

By considering the affine version of strong geometries arising from a set of points X in the space, we are able to give a positive answer to a strong geometry version of Las Vergnas’ question, in Section 5. More conveniently, the result is stated in the following equivalent way.

Theorem 1. *Let $X = (x_0, \dots, x_{n-1})$ and $X' = (x'_0, \dots, x'_{n-1})$ be two n -tuples of points in \mathbb{R}^3 in general position. Let $S\text{Geom}_{\text{Aff}}(X)$ and $S\text{Geom}_{\text{Aff}}(X')$ be the strong geometries associated to X and X' respectively. If $S\text{Geom}_{\text{Aff}}(X)$ is isomorphic to $S\text{Geom}_{\text{Aff}}(X')$ then K_X is isotopic to $K_{X'}$.*

Since the chirotope of $M_{\text{Wedge}}(X)$ determines the chirotope of $M_{\text{Lin}}(X)$ in dimension 4 (see Corollary 3) then the following result is a straightforward consequence of Theorem 1.

Corollary 1. *Let $X = (x_0, \dots, x_{n-1})$ and $X' = (x'_0, \dots, x'_{n-1})$ be two n -tuples of points in \mathbb{R}^3 in general position. If $M_{\text{Wedge}}(X)$ is isomorphic to $M_{\text{Wedge}}(X')$ then K_X is isotopic $K_{X'}$.*

In order to obtain Theorem 1, we prove that *knotoids* are determined by their Gauss diagram (see Lemma 3). The arguments for the latter are extended to show that *graphoids* are also determined by their Gauss diagram (see Lemma 4). This allows us to show, in Section 4, that *linear spatial graphs* are determined by their corresponding strong geometries as well (see Theorem 3).

2. ORIENTED MATROID PRELIMINARIES

For general background in oriented matroid theory we refer the reader to the book [4]. An *oriented matroid* $M = (E, \chi)$ of rank r is a finite set $E = \{1, \dots, n\}$ together with a function $\chi: E^r \rightarrow \{-1, 0, 1\}$, called *chirotope* verifying the following conditions

(CH0) χ is not always zero,

(CH1) χ is *alternating*, that is, for all $\{i_1, \dots, i_r\} \subset E$ and all $\sigma \in \mathfrak{S}_r$, we have

$$\chi(i_{\sigma(1)}, \dots, i_{\sigma(r)}) = \epsilon(\sigma)\chi(i_1, \dots, i_r),$$

(CH3) for all $\{i_1, \dots, i_r\}, \{j_1, \dots, j_r\} \subset E$ such that

$$\chi(j_k, i_2, \dots, i_r)\chi(j_1, \dots, j_{k-1}, i_1, j_{k+1}, \dots, j_r) \geq 0$$

for all k , then

$$\chi(i_1, \dots, i_r)\chi(j_1, \dots, j_r) \geq 0.$$

Let $1 \leq d \leq n$ be integers. To each configuration of vectors $X = (\mathbf{x}_1, \dots, \mathbf{x}_n) \in (\mathbb{R}^d)^n$, we may associate an oriented matroid $M = (E, \chi)$ of rank d by taking

$$\chi(i_1, \dots, i_d) = \Delta(\mathbf{x}_{i_1}, \dots, \mathbf{x}_{i_d}) \in \{-1, 0, 1\}.$$

where $\Delta = \text{sign} \circ \det$, that is, the sign of the determinant.

M is called *linear* or *vectorial* and it is denoted by $M_{\text{Lin}}(X)$.

We may also associate an oriented matroid $M = (E, \chi)$ of rank $r(M) = d + 1$ to a configuration of points $X = \{x_1, \dots, x_n\}$ in the affine space \mathbb{R}^d by taking

$$\chi(i_1, \dots, i_d) = \Delta \begin{pmatrix} 1 & \cdots & 1 \\ x_{i_1} & \cdots & x_{i_d} \end{pmatrix}.$$

M is called *affine* and it is denoted by $M_{\text{Aff}}(X)$.

We notice that we can pass from affine to linear matroids by considering the inclusion

$$\text{in} : \mathbb{R}^d \simeq \{1\} \times \mathbb{R}^d \subset \mathbb{R}^{d+1}.$$

We may thus write \mathbf{x} instead of x to distinguish vectors from points. From now on, when we refer \mathbb{R}^d as *affine space*, we mean that it is included in \mathbb{R}^{d+1} as $\{1\} \times \mathbb{R}^d$.

Let us recall that a set $P = \{p_1, \dots, p_n\}$ of $n \geq d+2$ points in \mathbb{R}^d always admits a *Radon partition*, that is, a partition $P = A \sqcup B$ such that $\text{conv}(\{p_i \mid p_i \in A\}) \cap \text{conv}(\{p_i \mid p_i \in B\}) \neq \emptyset$. It is known that a circuit $C = C^+ \cup C^-$ of an affine oriented matroid associated to a set of points $\{y_1, \dots, y_n\}$ corresponds to a minimal Radon partition, that is, $\text{conv}(\{y_i \mid i \in C^+\}) \cap \text{conv}(\{y_i \mid i \in C^-\}) \neq \emptyset$. If (x_1, \dots, x_{d+1}) is generic then a Radon partition of $\{x_1, \dots, x_{d+2}\}$ admits both x_{d+1} and x_{d+2} in either A or B if and only if $\chi(x_1, \dots, x_d, x_{d+1}) = -\chi(x_1, \dots, x_d, x_{d+2})$. Therefore, Radon's partitions can be recovered from the chirotope.

3. WEDGE MATROIDS

We shall first discuss the construction of wedge oriented matroids for $d = 2$ for a better comprehension. We then treat the general case $d \geq 3$.

3.1. Planar case. Let X be a set of points in \mathbb{R}^2 . As mentioned above, strong geometries intend to capture more geometric information than ordinary chirotopes, specifically, the relative positions of triples of lines generated by points in X . As explained above, it will be more convenient to consider X as included in \mathbb{R}^3 . Since we are only interested in computing signs of multi-linear expressions then we do not worry about the norm of the vectors in \mathbb{R}^3 . Therefore, the points in X will be associated to vectors living in $\mathbb{R}^3/(\mathbb{R}_+)$ which is $\mathbb{S}^d \cup \{0\}$.

Let x and y be two points in the affine space $\mathbb{R}^2 \subset \mathbb{R}^3$. Let $l_{x,y}$ be the equator arising from the intersection of the (oriented) plane $h_{x,y}$ spanned by x and y and \mathbb{S}^2 . Let \mathbf{x} and \mathbf{y} be the vectors on $l_{x,y}$ arising from intersection of \mathbb{S}^2 and the line segments $[0, x]$ and $[0, y]$ respectively. Equator $l_{x,y}$ is oriented from \mathbf{x} to \mathbf{y} , see Figure 2.

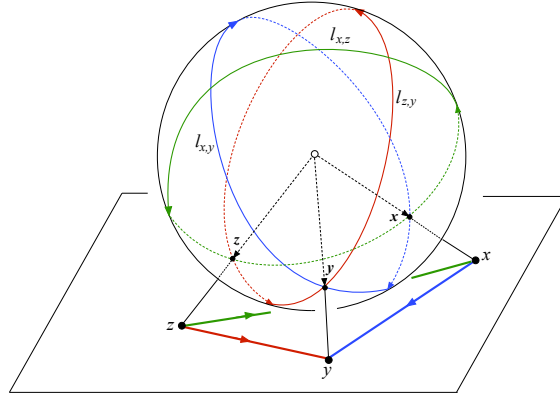


FIGURE 2. Unit vectors associated to points in the plane.

If we write \wedge for the image of \times in $\mathbb{R}^3/(\mathbb{R}_+)$ then the equator $l_{x,y}$ is parametrized by its normal positive vector given by the product $\mathbf{x} \wedge \mathbf{y}$. In the degenerate case, we consider the 0 vector to be the equator between two equal or antipodal points, see Figure 3.

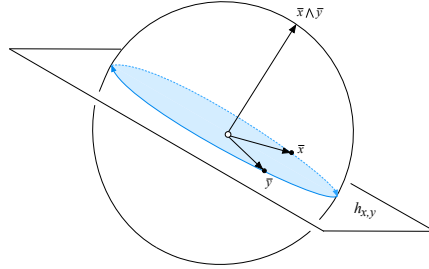


FIGURE 3

Remark 1. Let l be an oriented equator of \mathbb{S}^2 with positive normal vector \mathbf{v}_l and let l^+ (resp. l^-) be the positive (resp. negative) half-sphere delimited by l . Let \mathbf{p} be a vector in \mathbb{S}^2 . Then,

$$\mathbf{p} \in \begin{cases} l^+ & \text{if } \langle \mathbf{v}_l, \mathbf{p} \rangle > 0, \\ l^- & \text{if } \langle \mathbf{v}_l, \mathbf{p} \rangle < 0, \\ l & \text{if } \langle \mathbf{v}_l, \mathbf{p} \rangle = 0. \end{cases}$$

4

where $\langle \mathbf{u}, \mathbf{v} \rangle$ denotes the scalar product of vectors \mathbf{u} and \mathbf{v} .

Let x, y and z be points in the affine space. We commonly interpret $\Delta \begin{pmatrix} 1 & 1 & 1 \\ x & y & z \end{pmatrix}$ as indicating whether z lies on the positive or negative half-space delimited by the line from x to y . Similarly, this sign is also given by either

$$(1) \quad \Delta(\mathbf{x}, \mathbf{y}, \mathbf{z}) = \text{sign}(\langle \mathbf{x} \wedge \mathbf{y}, \mathbf{z} \rangle),$$

or the sign of the half-sphere delimited by the equator from \mathbf{x} to \mathbf{y} that contains \mathbf{z}

These observations serve as a guideline for a natural definition of the combinatorics of a tuple of oriented equators. Indeed, in affine geometry there are numerous ways that three oriented lines may meet, see Figure 4 while generic triplets of oriented equators can only be of two combinatorial types, see Figure 5.

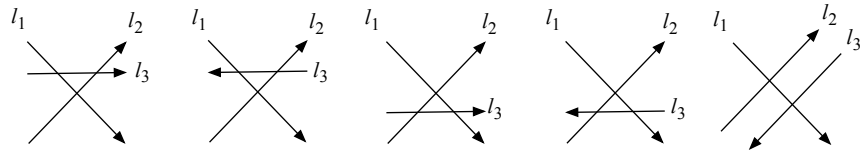


FIGURE 4. Some of the non-isotopic triplets of oriented lines.

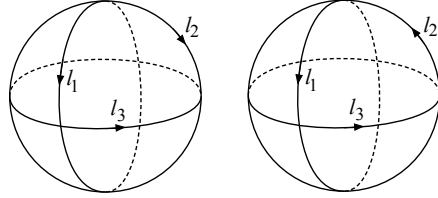


FIGURE 5. Positive and negative triplets of equators.

Let l_1 and l_2 be two equators and let \mathbf{v}_1 and \mathbf{v}_2 be the normal vectors of the corresponding hyperplanes supporting l_1 and l_2 respectively. If l_1 and l_2 are *colinear*, i.e. equal or opposite, then the sign associated to any triple (l_1, l_2, l) is always 0. Otherwise, they meet at two antipodal points p and $-p$, in this case, $\mathbf{v}_1 \wedge \mathbf{v}_2$ is one of these points, we call it *positive intersection*, see Figure 6.

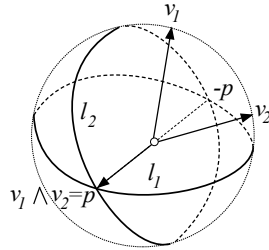


FIGURE 6

We thus have that a third equator l_3 admits either p or $-p$ on its positive half-sphere (the other in the negative half-sphere). Analogously to the dual case above (1), we define the sign associated to a triple of equators l_1, l_2 and l_3 as

$$(2) \quad \text{sign}(l_1, l_2, l_3) := \text{sign}(\langle \mathbf{v}_1 \wedge \mathbf{v}_2, \mathbf{v}_3 \rangle).$$

This leads us to define a chirotope χ_Λ on the set of equators by

$$\chi_\Lambda(i, j, k) := \text{sign}(l_i, l_j, l_k).$$

We call χ_Λ a *wedge* chirotope.

Note that if $l_i = \mathbf{x}_i \wedge \mathbf{y}_i$, $l_j = \mathbf{x}_j \wedge \mathbf{y}_j$ and $l_k = \mathbf{x}_k \wedge \mathbf{y}_k$, then we also have

$$(3) \quad \chi_\Lambda(i, j, k) = \Delta((\mathbf{x}_i \wedge \mathbf{y}_i) \wedge (\mathbf{x}_j \wedge \mathbf{y}_j), \mathbf{x}_k, \mathbf{y}_k).$$

3.2. General setting. We shall generalize the wedge chirotope to higher dimensions. To this end, we use the natural generalization of the cross product to higher dimension.

Let $d \geq 2$ and let $X = (\mathbf{x}_1, \dots, \mathbf{x}_d)$ be a d -tuple of vectors in \mathbb{R}^{d+1} (or in \mathbb{S}^d). If the family $(\mathbf{x}_1, \dots, \mathbf{x}_d)$ is independent then we define $\alpha(X)$ to be the (norm 1) $(d+1)$ -dimensional vector orthogonal to all \mathbf{x}_i 's (i.e., orthogonal to the hyperplane $h(X)$ spanned by the \mathbf{x}_i 's) and such that $\det(\mathbf{x}_1, \dots, \mathbf{x}_d, \alpha(X)) > 0$. We call $\alpha(X)$ an *hyperplane-vector*. If $(\mathbf{x}_1, \dots, \mathbf{x}_d)$ is dependent then we set $\alpha(X) = \mathbf{0}$ (in this case the hyperplane vector is *degenerate*).

Let $\mathcal{H} = \{h(I) \mid I \in [n]^d\}$. We may also suppose that the elements in \mathcal{H} are ordered, that is, if $h_i = h(I)$ and $h_j = h(J)$ then $h_i < h_j$ if $I < J$ (in lexicographic order).

Let $\Lambda(X)$ be the family of all hyperplane-vectors, that is,

$$\Lambda(X) = \left(\alpha(X_I) \right)_{I \in [n]^d}$$

For short, we may write $\Lambda(X) = \left(\alpha(I) \right)_{I \in [n]^d}$.

We define the *wedge oriented matroid*, denoted by $M_{\text{Wedge}}(X)$, as the oriented matroid $M_{\text{Lin}}(\Lambda(X))$, that is, the $(d+1)$ -rank oriented matroid with base set $[n]^d$ and with chirotope function χ_Λ verifying

$$\chi_\Lambda(I_1, \dots, I_{d+1}) = \Delta(\alpha(I_1), \dots, \alpha(I_{d+1}))$$

for $I_1, \dots, I_{d+1} \in [n]^d$.

Similarly as in the 2-dimensional case (i.e., rank 3), in the same flavor as Equation (3), we have the following result which is a straight consequence of the definition of α .

Lemma 1. *Let X_1, \dots, X_d, Y be $(d+1)$ d -tuples of vectors in \mathbb{R}^d and let $Y = (\mathbf{y}_1, \dots, \mathbf{y}_d)$. Then,*

$$\begin{aligned} \Delta(\alpha(X_1), \dots, \alpha(X_d), \alpha(Y)) &= \text{sign}(\langle \alpha(X_1), \dots, \alpha(X_d), \alpha(Y) \rangle) \\ &= \Delta(\alpha(\alpha(X_1), \dots, \alpha(X_d), \mathbf{y}_1, \dots, \mathbf{y}_d)). \end{aligned}$$

We define the *strong geometry* associated to X , denoted by $\text{SGeom}_{\text{Lin}}(X)$, as the structure composed by the couple $(M_{\text{Lin}}(X), M_{\text{Wedge}}(X))$. We may also consider the affine version $\text{SGeom}_{\text{Aff}}(X) = (M_{\text{Aff}}(X), M_{\text{Wedge}}(\text{in}(X)))$. Strong geometry will determine helpful complementary geometric information on the set X . Moreover, the chirotopes χ and χ_Λ are closely related as it is highlighted in the following two propositions.

Proposition 1. *Let $P = \{p_a, p_b, p_c, p_x, p_y\}$ be points in the affine space $\mathbb{R}^2 \subset \mathbb{R}^3$. Let h_1, h_2 and h_3 be the planes spanned by the couples of 3-dimensional vectors $I_1 = (\mathbf{p}_a, \mathbf{p}_b)$, $I_2 = (\mathbf{p}_a, \mathbf{p}_c)$ and $I_3 = (\mathbf{p}_x, \mathbf{p}_y)$ respectively. Recall that $\alpha(I_1) = \mathbf{p}_a \wedge \mathbf{p}_b$, $\alpha(I_2) = \mathbf{p}_a \wedge \mathbf{p}_c$ and $\alpha(I_3) = \mathbf{p}_x \wedge \mathbf{p}_y$. Then,*

$$(4) \quad \chi_\Lambda(I_1, I_2, I_3) = \chi(a, b, c)\chi(a, x, y).$$

Proof. If $\chi(a, b, c) = 0$ then the equality (4) can be easily checked. Let us thus suppose that $\chi(a, b, c) \neq 0$, that is, p_a, p_b and p_c are points in generic position. Since \mathbf{p}_a is in both $l_1 = \mathbf{p}_a \wedge \mathbf{p}_b$ and $l_2 = \mathbf{p}_a \wedge \mathbf{p}_c$, then the positive intersection of equators l_1 and l_2 is either p_a if $\chi(a, b, c) = +1$ or $-p_a$ if $\chi(a, b, c) = -1$ (if $\chi(a, b, c) = 0$ then $\mathbf{p}_a \wedge \mathbf{p}_b$ and $\mathbf{p}_a \wedge \mathbf{p}_c$ are colinear). This is due to the fact there is only one isotopy class of positive triples of vectors.

We have that (4) can be thus stated as

$$(\mathbf{p}_a \wedge \mathbf{p}_b) \wedge (\mathbf{p}_a \wedge \mathbf{p}_c) = \chi(a, b, c) \mathbf{p}_a.$$

Combining this equality with

$$\chi_\Lambda(I_1, I_2, I_3) = \text{sign}\left(\langle (\mathbf{p}_a \wedge \mathbf{p}_b) \wedge (\mathbf{p}_a \wedge \mathbf{p}_c), (\mathbf{p}_x \wedge \mathbf{p}_y) \rangle\right)$$

the desired equality follows, see Figure 7. \square

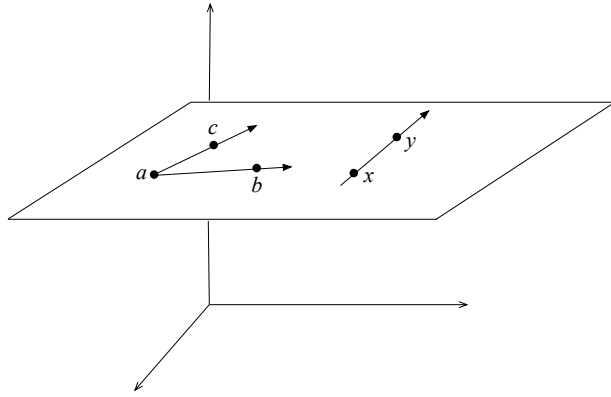


FIGURE 7. A visual explanation of Proposition 1 in the affine setting.

A consequence of Proposition 1 is the following

Corollary 2. *Let X and X' be two n -tuples in \mathbb{R}^3 . If $M_{\text{Wedge}}(X)$ is isomorphic to $M_{\text{Wedge}}(X')$ then the chirotopes of $M_{\text{Lin}}(X)$ and $M_{\text{Lin}}(X')$ are either equal or opposite.*

Proof. Suppose that X, X' have the same wedge chirotope. By applying Proposition 1 to $(x, y) = (b, c)$, we obtain that X and X' agree on triples having sign equal to 0.

Now, again according to Proposition 1, X and X' agree on whether two bases sharing some element have equal or opposite orientations. This implies that they also agree for any pair of bases $(x_{i_1}, x_{i_2}, x_{i_3})$ and $(x_{i_4}, x_{i_5}, x_{i_6})$, since, according to the matroid basis exchange property, we can pass from $(x_{i_1}, x_{i_2}, x_{i_3})$ to $(x_{i_4}, x_{i_5}, x_{i_6})$ through (x_{i_1}, x_{i_2}, x_k) for some $k \in \{i_4, i_5, i_6\}$. This shows that the chirotopes are either equal or opposite. \square

We notice that, conversely, two opposite configurations have the same wedge chirotope.

We shall extend Proposition 1 to affine space \mathbb{R}^3 . To this end, we introduce the *witness chirotope* but, before doing so, let us first briefly discuss our motivation behind this new structure.

The main issue is that, instead of studying knots through their diagrams (orthogonal projections in the plane), we rather consider a projection of the knot radially to a sphere, say with center ω . Therefore, given $x_1, \dots, x_n \in \mathbb{R}^3$, we are interested in the linear geometry of the $x_1 - \omega, \dots, x_n - \omega \in \mathbb{R}^3$ (notice that the rank decreases by one). In this setting, the most relevant piece of information in the knot sphere diagram will be given by the strong geometry of such configuration (that is, a strong geometry witnessed by ω). As we will see in Proposition ??, the

latter is induced by the strong geometry of the initial configuration since affine oriented hyperplanes $\alpha(\omega, \mathbf{x}_1, \mathbf{y}_1), \alpha(\omega, \mathbf{x}_2, \mathbf{y}_2), \alpha(\omega, \mathbf{x}_3, \mathbf{y}_3)$ meet either positively or negatively at ω depending on whether ω sees the oriented lines $(\mathbf{x}_1, \mathbf{y}_1), (\mathbf{x}_2, \mathbf{y}_2), (\mathbf{x}_3, \mathbf{y}_3)$ as a positive or negative triple. Notice that Proposition 1 is the rewording of the preceding remark in lower rank, although the strong geometry is hidden by the fact that, in rank 2, it is the same as the usual chirotope.

The above discussion naturally leads us to define the *witness* chirotope as follows. Let ω, x_1, \dots, x_n be a configuration of points in affine space \mathbb{R}^d , we note χ_ω the linear chirotope of the vector configuration $(x_i - \omega)_{i \in [n]}$. Of course, since

$$\begin{vmatrix} 1 & 1 & \dots & 1 \\ \omega & x_{i_1} & \dots & x_{i_d} \end{vmatrix} = \begin{vmatrix} 1 & 0 & \dots & 0 \\ \omega & x_{i_1} - \omega & \dots & x_{i_d} - \omega \end{vmatrix} = |x_{i_1} - \omega, \dots, x_{i_d} - \omega|,$$

then $\chi_\omega(\cdot, \dots, \cdot) = \chi(\omega, \cdot, \dots, \cdot)$, see figure 8.

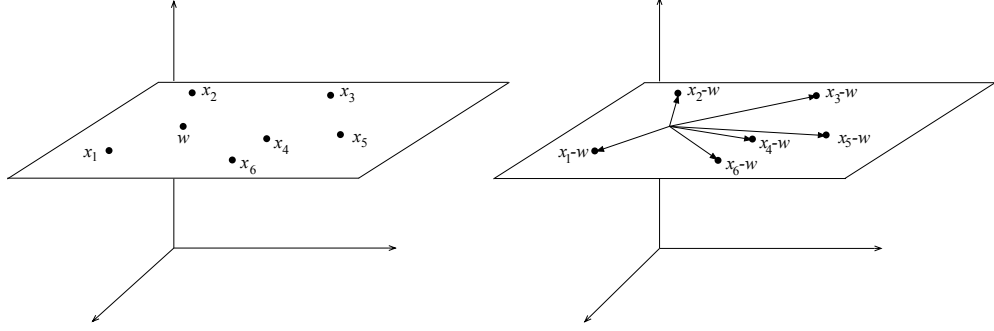


FIGURE 8. (Left) Affine oriented matroid of rank 3 associated to points ω, x_1, \dots, x_6 . (Right) Witness oriented matroid of rank 2 associated to vectors $\mathbf{x}_1 - \omega, \dots, \mathbf{x}_6 - \omega$.

Since we want to study ‘witnessed strong geometry’, it is also natural to define $\chi_{\omega, \wedge}$ on $(x_i) \in (\mathbb{R}^d)^n$ as the rank d , linear wedge chirotope of $(x_i - \omega)_{i \in [n]}$.

In order to present clearer and more proper proofs, it is convenient to have a second approach for the definition of a ‘witness chirotope’, this time starting and ending in a linear space and, of course, coinciding with the above definition.

Since $x \mapsto x - \omega$ simply acts on $\{1\} \times \mathbb{R}^d$ as the projection on $\{0\} \times \mathbb{R}^d$ with kernel $\langle \omega \rangle$, the most obvious replacement is the orthogonal projection π_{ω^\perp} on ω^\perp . In order to be consistent with the previous definition, we orient ω^\perp such that positive bases of ω^\perp are the (b_1, \dots, b_{d-1}) such that $(\omega, b_1, \dots, b_{d-1})$ is a positive basis of \mathbb{R}^d . We thus have that the linear equivalent of the above definition can be obtained by setting the witnessed strong geometry of X witnessed by ω as the strong geometry of $\pi_{\omega^\perp}(X)$ (in $\omega^\perp \simeq \mathbb{R}^{d-1}$).

Although both definitions seem to be the most natural ones, it is not immediate to convince one-self that they coincide. Indeed, if all the ω, x_i live in $\{1\} \times \mathbb{R}^3$, then the map $x \mapsto x - \omega$ acts on the x_i as the projection on $\{0\} \times \mathbb{R}^3$ with kernel ω , which is not necessarily the orthogonal projection (unless $\omega = e_1$ of course)

Let us check that both projections of the point configurations do have the same strong geometry.

Lemma 2. Let H_1, H_2 be two hyperplanes of \mathbb{R}^d not containing $\omega \neq 0$, and let π_1, π_2 the projections with kernel $\langle \omega \rangle$ and respective images H_1, H_2 . Suppose further that the H_i are oriented such that a positive base (b_1, \dots, b_{d-1}) of H_i induces a positive base $(\omega, b_1, \dots, b_{d-1})$ of \mathbb{R}^d . Then for any $X \in (\mathbb{R}^d)^n$, $\pi_1(X)$ and $\pi_2(X)$ have the same strong geometry.

Proof. We first notice that the $\pi_i(X)$ only differ by a positive isomorphism. Indeed the composition $H_1 \hookrightarrow \mathbb{R}^d \rightarrow H_2$ of the canonical inclusion and the projection π_2 is a linear map between vector spaces of same dimensions, with trivial kernel, that is, an isomorphism. It also sends a basis (b_1, \dots, b_{d-1}) to some $(b_1 - \lambda_1 \omega, \dots, b_{d-1} - \lambda_{d-1} \omega)$, and since $|\omega, b_1 - \lambda_1 \omega, \dots, b_{d-1} - \lambda_{d-1} \omega| = |\omega, b_1, \dots, b_{d-1}|$, it is a positive isomorphism. We claim that a positive isomorphism preserve the strong geometry.

Firstly, notice that for a family $(h_i)_{i \in I}$ of hyperplanes and $(v_i)_{i \in I}$ its family of normal vectors, a vector v is orthogonal to all v_i if and only if it belongs to all h_i . But a $((d-1) \times (d-2))$ -tuple $(x_{i,j})$ verifies $\Delta(\alpha(x_{1,1}, \dots, x_{1,d-2}), \dots, \alpha(x_{d-1,1}, \dots, x_{d-1,d-2})) = 0$ if and only if the $\alpha(x_{i,1}, \dots, x_{i,d-2})$ are linearly dependent, or equivalently, if there is a non-zero vector orthogonal to all of them. Therefore, $\Delta(\alpha(x_{1,1}, \dots, x_{1,d-2}), \dots, \alpha(x_{d-1,1}, \dots, x_{d-1,d-2})) = 0$ if and only if $\dim(\bigcap_i \langle x_{i,1}, \dots, x_{i,d-2} \rangle) \neq 0$. Now acting on the $x_{i,j}$ by isomorphism does not change this dimension, therefore

$$\Delta(\alpha(x_{1,1}, \dots, x_{1,d-2}), \dots, \alpha(x_{d-1,1}, \dots, x_{d-1,d-2})) = 0$$

if and only if

$$\Delta(\alpha(\phi(x_{1,1}), \dots, \phi(x_{1,d-2})), \dots, \alpha(\phi(x_{d-1,1}), \dots, \phi(x_{d-1,d-2}))) = 0$$

for any isomorphism ϕ .

Take now a positive isomorphism ϕ . Since the group of positive isomorphisms is path connected, we have a continuous path ϕ_t of (positive) isomorphisms such that $\phi_0 = \text{id}$, $\phi_1 = \phi$. If we had, say

$$\Delta(\alpha(x_{1,1}, \dots, x_{1,d-2}), \dots, \alpha(x_{d-1,1}, \dots, x_{d-1,d-2})) > 0$$

and

$$\Delta(\alpha(\phi(x_{1,1}), \dots, \phi(x_{1,d-2})), \dots, \alpha(\phi(x_{d-1,1}), \dots, \phi(x_{d-1,d-2}))) < 0$$

on some $(x_{i,j})$, then there would be some $t \in (0, 1)$ such that

$$\Delta(\alpha(\phi_t(x_{1,1}), \dots, \phi_t(x_{1,d-2})), \dots, \alpha(\phi_t(x_{d-1,1}), \dots, \phi_t(x_{d-1,d-2}))) < 0,$$

but, we just saw that this cannot happen. Hence,

$$\Delta(\alpha(x_{1,1}, \dots, x_{1,d-2}), \dots, \alpha(x_{d-1,1}, \dots, x_{d-1,d-2})) = \Delta(\alpha(\phi(x_{1,1}), \dots, \phi(x_{1,d-2})), \dots, \alpha(\phi(x_{d-1,1}), \dots, \phi(x_{d-1,d-2}))).$$

Implying that positive isomorphisms preserve the strong geometry, as desired. \square

We have thus checked that the natural definition of witnessed strong geometry from affine space to linear space coincides with the definition from linear space to linear space. A rigorous formulation of the latter is given by the following generalized version of Proposition 1.

Theorem 2. Let $\omega, x_{1,1}, \dots, x_{1,d-2}, \dots, x_{d-1,d-2}, y_1, \dots, y_{d-1} \in \mathbb{R}^d$, with $\omega \neq 0$. Let us denote by $\tilde{\alpha}$ and $\tilde{\Delta}$ the α and Δ functions associated with the oriented hyperplane ω^\perp . Then, we have that

$$\begin{aligned} & \Delta(\alpha(\omega, x_{1,1}, \dots, x_{1,d-2}), \dots, \alpha(\omega, x_{d-1,1}, \dots, x_{d-1,d-2}), \alpha(y_1, \dots, y_{d-1})) \\ &= (-1)^{d+1} \tilde{\Delta}(\tilde{\alpha}(x_{1,1}, \dots, x_{1,d-2}), \dots, \tilde{\alpha}(x_{d-1,1}, \dots, x_{d-1,d-2})) \Delta(\omega, y_1, \dots, y_{d-1}) \end{aligned}$$

Proof. The proof runs similarly as the one for Proposition 1. The point is that the left hand term is the relative position between the hyperplane represented by $\alpha(y_1, \dots, y_{d-1})$ and the positive intersection $\alpha(v_1, \dots, v_{d-1})$ of the hyperplanes represented by the $v_i = \alpha(\omega, x_{i,1}, \dots, x_{i,d-2})$. The proof consists in showing that the latter is precisely

$$(-1)^{d+1} \tilde{\Delta}(\tilde{\alpha}(x_{1,1}, \dots, x_{1,d-2}), \dots, \tilde{\alpha}(x_{d-1,1}, \dots, x_{d-1,d-2}))\omega.$$

Since the hyperplanes represented by the $\alpha(\omega, x_{i,1}, \dots, x_{i,d-2})$ all contain ω , their positive intersection $\alpha(v_1, \dots, v_{d-1})$ is some $\eta\omega$, with $\eta \in \{-1, +1\}$ (unless it is trivial, in which case the proof is straightforward). By definition,

$$\Delta(\alpha(\omega, x_{1,1}, \dots, x_{1,d-2}), \dots, \alpha(\omega, x_{d-1,1}, \dots, x_{d-1,d-2}), \eta\omega) = 1$$

so we simply want to compute

$$\eta = \Delta(\alpha(\omega, x_{1,1}, \dots, x_{1,d-2}), \dots, \alpha(\omega, x_{d-1,1}, \dots, x_{d-1,d-2}), \omega).$$

Note that $\alpha(\omega, x_{i,1}, \dots, x_{i,d-2}) = \tilde{\alpha}(p(x_{i,1}), \dots, p(x_{i,d-2}))$ where p denotes the orthogonal projection on ω^\perp (because a vector orthogonal to ω is orthogonal to some x if and only if it is orthogonal to $p(x)$, and because the choice of convention for the orientation of ω^\perp was made to have no "–" sign appear here).

Therefore, we have

$$\begin{aligned} \eta &= \Delta(\tilde{\alpha}(p(x_{1,1}), \dots, p(x_{1,d-2})), \dots, \tilde{\alpha}(p(x_{d-1,1}), \dots, p(x_{d-1,d-2})), \omega) \\ &= (-1)^{d+1} \Delta(\omega, \tilde{\alpha}(p(x_{1,1}), \dots, p(x_{1,d-2})), \dots, \tilde{\alpha}(p(x_{d-1,1}), \dots, p(x_{d-1,d-2}))) \\ &= (-1)^{d+1} \tilde{\Delta}(\tilde{\alpha}(x_{1,1}, \dots, x_{1,d-2}), \dots, \tilde{\alpha}(x_{d-1,1}, \dots, x_{d-1,d-2})) \end{aligned}$$

the last equality is by definition of $\tilde{\Delta}$. The desired equality follows. \square

Let us rephrase Theorem 2 in terms of abstract chirotope. We restrict ourselves to the rank 4 case and state it in terms of projection from affine space (handy for the knot's application).

Proposition 2. *Let $n \geq 1$ be an integer and let $X = (\omega = x_0, x_1, \dots, x_n)$ be a tuple of points in \mathbb{R}^3 .*

Let $i_0 = 0, i_1, \dots, i_9 \in [n]^9$ and let $I_1 = (i_0, i_1, i_2)$, $I_2 = (i_0, i_3, i_4)$, $I_3 = (i_0, i_5, i_6)$ and $J = (i_7, i_8, i_9)$. Let $a_1 = (i_1, i_2)$, $a_2 = (i_3, i_4)$, $a_3 = (i_5, i_6)$. Then,

$$\chi_{\wedge}(I_1, I_2, I_3, J) = -\chi_{\Lambda, \omega}(a_1, a_2, a_3)\chi(i_0, i_7, i_8, i_9)$$

where χ_{Λ} , χ and $\chi_{\wedge, \omega}$ are the chirotopes of the rank 4 matroids $M_{\text{Wedge}}(\text{in}(X))$ and $M_{\text{Lin}}(\text{in}(X)) = M_{\text{Aff}}(X)$ and the rank 3 matroid $M_{\text{Wit}_{\omega}}(X)$ respectively.

Here, $M_{\text{Wit}_{\omega}}(X)$ is the witness oriented matroid of the configuration of points in the sphere centered at ω obtained by radial projection of X .

Proof. Since the norms of the vectors are not taken into account in a linear matroid and they can be projected on the sphere then the desired equality is simply expressing Theorem 2 through one of the equivalent definitions of wedge chirotope (by using Lemma 2). \square

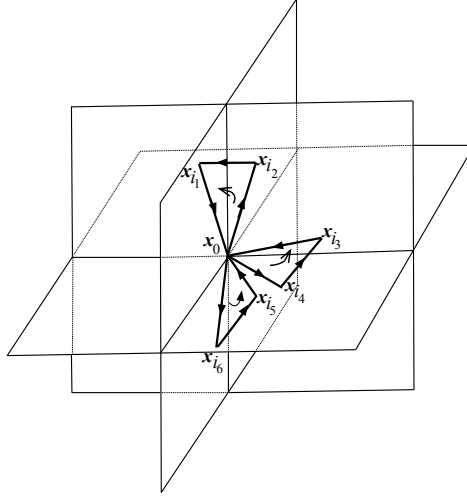


FIGURE 9. This figure sums up the situation of Proposition 2. The three hyperplanes meet positively or negatively at x_0 depending on the sign of the triplet of lines witnessed by x_0 .

Corollary 3. *Let X and X' be two n -tuples in \mathbb{R}^4 . If $M_{\text{Wedge}}(X)$ and $M_{\text{Wedge}}(X')$ are isomorphic then $M_{\text{Lin}}(X)$ and $M_{\text{Lin}}(X')$ also are.*

Proof. According to Proposition 1, $\chi(a \wedge b, a \wedge c, b \wedge c) = \chi(a, b, c)^2$. By plugging this into the equality of Proposition 2, we obtain

$$\begin{aligned} \chi((\alpha(x, a, b), \alpha(x, a, c), \alpha(x, b, c), \alpha(a, b, c))) &= \chi_x(a, b, c)^2 \chi(x, a, b, c) \\ &= \chi(x, a, b, c)^2 \chi(x, a, b, c) \\ &= \chi(x, a, b, c). \end{aligned}$$

□

Corollaries 2 and 3 can be extended to higher dimension.

Corollary 4. *Let X and X' be two n -tuples in \mathbb{R}^d . If $M_{\text{Wedge}}(X)$ is isomorphic to $M_{\text{Wedge}}(X')$ then the chirotopes of $M_{\text{Lin}}(X)$ and $M_{\text{Lin}}(X')$ are equal if d is even and either equal or opposite if d is odd.*

The proof is also a consequence of Theorem 2 (analogue to the lower rank cases with some extra tedious indices manipulation).

4. GEOMETRIC KNOTS

Let us first recall a simple way to encode a knot diagram that enable to reconstruct an equivalent diagram from it.

4.1. Gauss code. A *Gauss code* of an oriented knot diagram with n crossings is constructed as follows. Label all the crossings of the diagram from 1 to n (in an arbitrary manner). The Gauss code is derived by walking the knot, starting at point P of the diagram (picked arbitrarily and other than a crossing). As we follow the diagram, we record the crossings we encounter, by writing down the labels preceded with an ‘O’ or ‘U’ to indicate whether the curve goes *Over* or *Under* strand, see Figure 10.

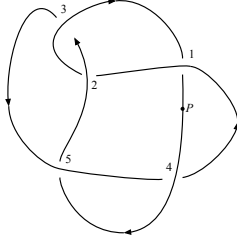


FIGURE 10. Knot 5_2 with Gauss code $O_4 U_5 O_2 U_3 O_5 U_4 O_1 U_2 O_3 U_1$.

In general, the Gauss code for a knot diagram cannot be used to reconstruct an equivalent diagram, but an extension of it will make the reconstruction possible. The *extended Gauss code* is a minor revision of Gauss code : as we encounter a given crossing, we record it as above and we also assign a sign depending on the handedness of the crossing. If it is *right-handed*, we assign positive; if it is *left-handed*, negative, see Figure 11.

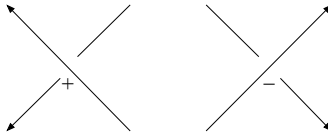


FIGURE 11. Positive and negative oriented crossings.

The extended Gauss code of the example illustrated in Figure 10 is given by

$$O_+4 U_+5 O_+2 U_+3 O_+5 U_+4 O_-1 U_+2 O_+3 U_-1.$$

A diagrammatic representation of an extended Gauss code is given by a *Gauss diagram* constructed as follows. Take an oriented circle with a base point chosen on the circle. Walk along the circle marking it with the labels for the crossings in the order of the Gauss code. Now draw chords between the points on the circle that have the same label. Orient each chord from the over crossing to the under crossing in the Gauss code. Mark each chord with + or - according to the sign of the corresponding crossing in the Gauss code. An example of the Gauss diagram for the knot 6_3 is given in Figure 12.

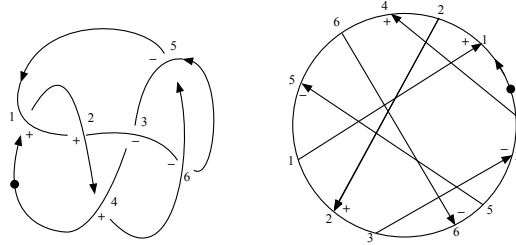


FIGURE 12. (Left) 6_3 with Gauss code $U_+1 O_+2 U_+4 O_-6 U_-5 O_+1 U_+2 O_-3 U_-6 O_-5 U_-3 O_+4$
(Right) Corresponding Gauss diagram.

It is known that a knot diagram on the sphere can be recovered uniquely (up to isotopy) from its Gauss diagram which can thus be considered as an alternative way to present knots. Unfortunately, not every picture which looks like a Gauss diagram is indeed a Gauss diagram of some knot. This is not easy to recognize, see [5].

A Gauss diagram can also be represented by an oriented line where the ends are identified and having oriented signed arcs corresponding to the chords, see en Figure 13.

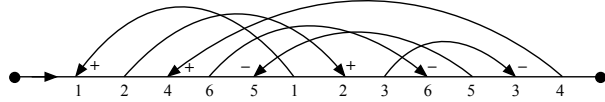


FIGURE 13. Line representation of the Gauss diagram illustrated in Figure 12.

4.2. Knotoids. *Knotoids* are variants of knots that were first introduced by Turaev in [20]. The idea is to consider diagrams of segments with endpoints. Contrarily to knots, they are only defined as equivalence classes of diagrams, since all embedding of the interval in \mathbb{R}^3 are ambient isotopic. More precisely, a *knotoid* is an equivalence class of *knotoid diagrams*. A *knotoid diagram* is the image of an application $[0, 1] \rightarrow \mathbb{R}^2$ that satisfies the usual properties of a knot diagram, that is, each point has at most two preimages, called crossings, and there is a finite number of such crossings; besides, crossings happen between two transversal strands. We further suppose that the endpoints do not lie on crossings. The equivalence relationship considered here is the one generated by planar isotopy and the usual Reidemeister moves ; endpoints are not allowed to cross strands.

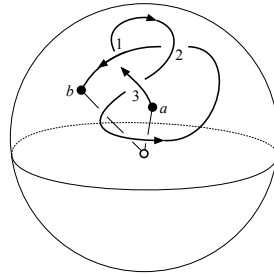


FIGURE 14. The knotoid called *line eight-figure*.

Similarly as we do for knots, we may associate to a knotoid diagram its Gauss diagram. Take an oriented segment, say S , with an initial and end points. Walk along S marking it with the labels for the crossings in the order they are encountered as walking through the knotoid from one end to the other. Now draw arcs between the marks on S that have the same label. Orient each arc from the over crossing to the under crossing in the knotoid. Mark each arc with + or - according to handedness' rule, see Figure 15.

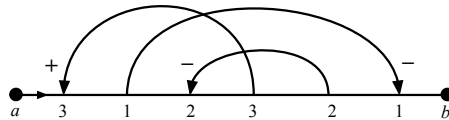


FIGURE 15. The Gauss diagram arising from knotoid given in Figure 14.

Lemma 3. *A knotoid diagram is determined by its Gauss diagram (up to a planar isotopy).*

Proof. A proof might follow by slightly adapting the classic procedure showing that Gauss diagrams determine knot diagrams given in [16]. Nevertheless, we propose a new approach. We will see that any face of the knotoid diagram can be determined by using the Gauss diagram. We shall show

that the set of faces (and whether two of them share an edge) in the knotoid diagram corresponds to the set of *valid* travels in the Gauss diagram.

Let us consider a walk W on the arcs on the boundary of a face (say, counterclockwise) in the knotoid diagram. Notice that we can run through an arc either following its direction or in opposite direction, see Figure 16.

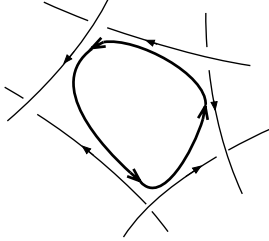


FIGURE 16. Walk around a boundary of a face.

We associate to W a travel T along the Gauss diagram. Turns of W at a crossing correspond to jumps in arrows (from head/tail to tail/head) and each arc in W corresponds to a piece of the oriented segment S (of the Gauss diagram). Travel T may follow or not the direction of S (depending on whether or not W follows the direction of the corresponding arc). Since W goes around a face then this correspondence obeys certain rules according to the sign of the crossing and from which strand (over/under) the walk comes from and goes to. These rules are illustrated in Figure 17.

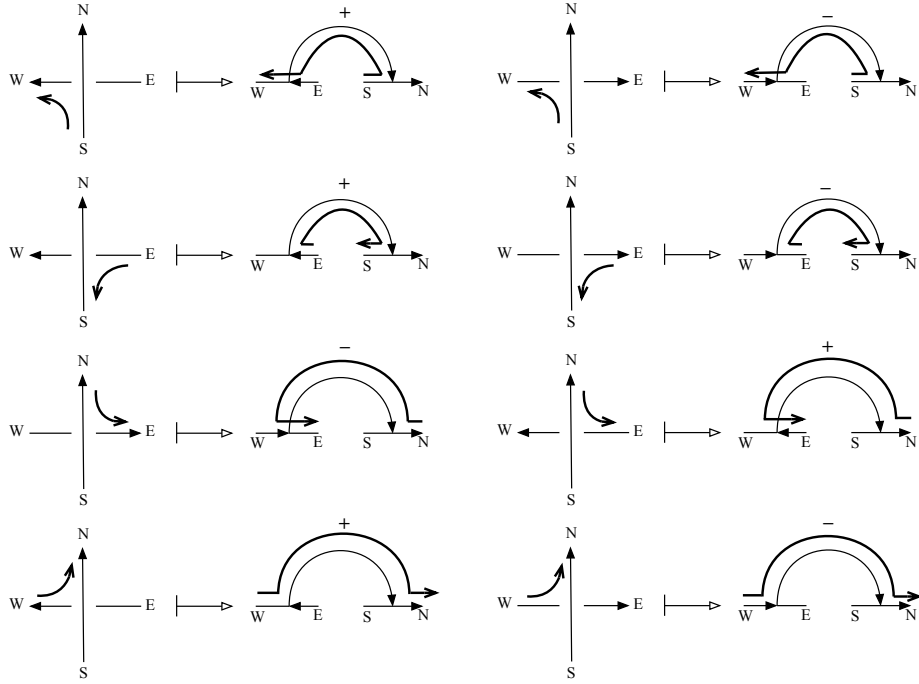


FIGURE 17. Local turnings of a walk around a crossing and the corresponding local travel in the Gauss diagram (in bold).

The travel T constructed this way is called a *valid* travel in the Gauss diagram. In fact, if the labels **North**, **South**, **East** and **West**, as well as the signs of each arrow in a Gauss diagram are

fixed then, a valid travel T verifies the rule :

$$\mathbf{N} \rightarrow \mathbf{E} \rightarrow \mathbf{S} \rightarrow \mathbf{W} \rightarrow \mathbf{N}$$

where $\mathbf{X} \rightarrow \mathbf{Y}$ means «go from \mathbf{X} to \mathbf{Y} ».

These rules on T force, by construction, that the corresponding walk W always turns «left» at each crossing, see Figure 18

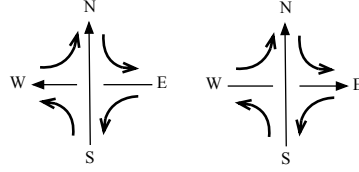


FIGURE 18. Turns of W induced by valid travels.

Therefore, W will be necessarily a walk of a face in the knotoid. Moreover, two valid travels sharing a same piece of S (with opposite direction) correspond to two faces sharing an edge.

Finally, we observe that a valid travel going through an end of the line goes back with opposite orientation, see Figure 19.

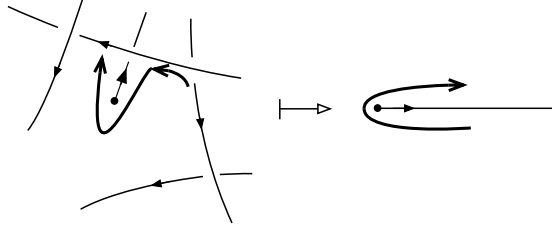


FIGURE 19. Walk of a face containing a degree one vertex and the corresponding travel.

□

4.3. Main result. Let $y_0 \in \mathbb{R}^3$ and let π_{y_0} be the radial projection emitting from y_0 to \mathbb{S}^2 , that is,

$$\begin{aligned} \pi_{y_0} : \mathbb{R}^3 \setminus \{y_0\} &\rightarrow \mathbb{S}^2 \\ y &\mapsto \frac{y-y_0}{\|y-y_0\|} \end{aligned}$$

Let K be a knot in \mathbb{R}^3 (not passing through y_0). We may associate to K a *sphere shadow* which is just the radial projection $\pi_{y_0}(K)$. We may suppose that such a shadow is regular in the sense that it avoids cusps and tangency points (this can be obtained by making some suitable local modifications to K without changing its type). Let z be a point in $\pi_{y_0}(K)$, suppose that

$$z = \pi_{y_0}(y_1) = \dots = \pi_{y_0}(y_k), \quad k \geq 1.$$

We say that z is a *simple intersection* point if $k = 2$ and a *multiple intersection* point if $k \geq 3$. We may avoid multiple intersection points by moving pieces of the shadow around z properly. As for standard knots, doing such a perturbation does not change the knot type, however, in our case we need slightly more. We have to make sure that the strong geometry captures the information determining the possible diagrams.

The set of possible perturbations is completely determined by the local type of the multiple intersection, that is, the order (say counterclockwise) in which the strands appear as we rotate

around the intersection point (because this determines the local diagram up to planar isotopy). Suppose that the strands are oriented inducing a ‘right’ and a ‘left’ side of the strand. Hence, each strand a_i partitions the other a_j , $j \neq i$ into two sets, those crossing a_i left-to-right and those crossing it right-to-left.

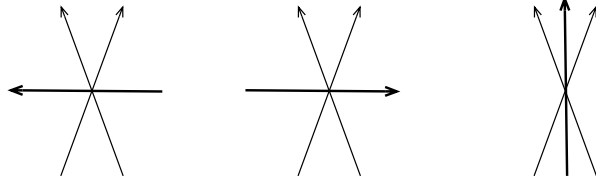


FIGURE 20. (Left) Two consecutive strands (bold strand crosses both right-to-left) (Center) Two consecutive strands (bold strand crosses both left-to-right) (Right) Two nonconsecutive strands (bold strand crosses left-to-right one of them and right-to-left the other).

We have that two strands are consecutive if and only if they partition the other strands in equal or opposite sets. Therefore, we simply need to know the sign of each crossing in order to know what all the possible local perturbation. This piece of information will be shown to be induced by the strong geometry.

If the reader is not comfortable with these local permutations, instead, a notion of knot diagram allowing multiple crossings could be defined. The reasoning to check that the strong geometry gives the information about the strands around such multiple crossings would be essentially the same as above.

Therefore, sphere shadows can be thought of as 4-regular maps (i.e., an embedding of a 4-regular planar graph into \mathbb{S}^2). A *spherical diagram* of K is obtained from such a shadow by endowing the under/over information to each vertex, see Figure 21.

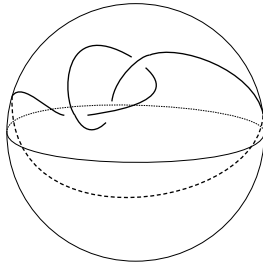


FIGURE 21. A spherical diagram of the Trefoil.

A spherical diagram is still a knot diagram of K in the usual sense. In particular, knots having isotopic spherical diagrams are isotopic.

We may now prove Theorem 1.

Proof of Theorem 1. Let $X = (x_0, \dots, x_{n-1})$ be tuple of points in \mathbb{R}^3 in general position. Let K be the polygonal knot formed by segments $[x_0, x_1] \cup [x_1, x_2] \cup \dots \cup [x_{n-1}, x_0]$. We show that $\text{SGeom}(X)$ determines uniquely the type of K . Let us consider the radial projection $\pi_{x_0}(K - \{x_0\})$ of $K \setminus \{x_0\}$ emitted from x_0 .

Remark 2. (a) π_{x_0} maps each semi-open interval $(x_0, x_1]$ and $(x_0, x_{n-1}]$ into a single point. We thus have that the corresponding spherical diagram induced by $\pi_{x_0}(K)$ is a knotoid, denoted by \mathcal{K} .

(b) Since K is polygonal with points in generic position then the shadow $\pi_{x_0}(K - \{x_0\})$ has no tangency point.

(c) $\pi_{x_0}(K)$ may have multiple intersection points. These can be fixed/modified as explained above.

We notice that any planar isotopy between knotoids can be extended to an isotopy of knots by fixing x_0 and keeping the segments $[x_{n-1}, x_0]$ and $[x_0, x_1]$ straight while doing the isotopy.

Therefore, by Lemma 3, it is enough to show that the Gauss diagram associated to knotoid \mathcal{K} is completely determined by $\text{SGeom}_{\text{Aff}}(X) = (M_{\text{Aff}}(X), M_{\text{Wedge}}(\text{in}(X)))$ (implying that K can also be uniquely reconstructed from such strong geometry). To this end, we show that $\text{SGeom}_{\text{Aff}}(X)$ determines the following two points.

(A) the pairs of arcs that intersect (and which one is over/under the other one) together with the corresponding sign,

(B) the order of the intersections (if more than one) along a given arc in \mathcal{K} .

For (A), let $\beta = \pi_{x_0}([x_i, x_{i+1}])$ and $\beta' = \pi_{x_0}([x_{i'}, x_{i'+1}])$ be two arcs in \mathcal{K} . Suppose that these arcs intersect in a simple point. Then, β is over β' if the Radon partition of the set $\{x_0, x_i, x_{i+1}, x_{i'}, x_{i'+1}\}$ is given by $\{x_0, x_i, x_{i+1}\} \sqcup \{x_{i'}, x_{i'+1}\}$, see Figure 22.

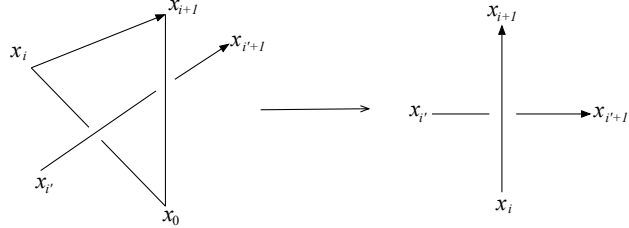


FIGURE 22. Radon partition and crossing in \mathcal{K} from the witness x_0 .

Furthermore, if arc $\pi_{x_0}([x_i, x_{i+1}])$ intersect arc $\pi_{x_0}([x_{i'}, x_{i'+1}])$ then the oriented arcs (from x_i to x_{i+1} and from $x_{i'}$ to $x_{i'+1}$) on the sphere meet at a positive crossing if and only if $\chi(x_i, x_{i+1}, x_0, x_{i'+1}) = +1$.

For (B), suppose that both arcs $\beta' = \pi_{x_0}([x_{i'}, x_{i'+1}])$ and $\beta'' = \pi_{x_0}([x_{i''}, x_{i''+1}])$ intersect arc $\beta = \pi_{x_0}([x_i, x_{i+1}])$. The order of the intersection, say from $\pi_{x_0}(x_i)$ to $\pi_{x_0}(x_{i+1})$ is given by the chirotope χ_{x_0} according with the rule given in Figure 23. We notice that, by Proposition 2, χ_{\wedge, x_0} can be completely determined from χ_{Λ} .

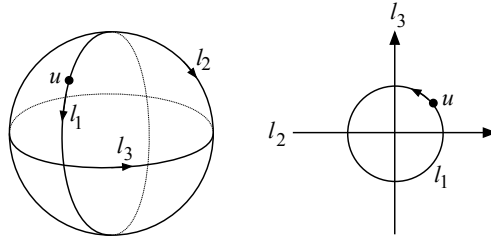


FIGURE 23. If $\chi_{x_0}(1, 2, 3) = +1$ then, by walking along l_1 following its direction, say from u , l_1 meets l_3 negatively, then l_2 positively, then l_3 positively and finally l_2 negatively.

Let $l_1 = i \wedge (i+1)$, $l_2 = i' \wedge (i'+1)$ and $l_3 = i'' \wedge (i''+1)$. Then, by following Figure 23 with $\chi_{x_0}(1, 2, 3) = +1$ we have that

$$\text{if } \beta \text{ crosses } \begin{cases} \beta' \text{ positively and } \beta'' \text{ positively then } \beta \text{ meets } \beta'' \text{ before } \beta', \\ \beta' \text{ positively and } \beta'' \text{ negatively then } \beta \text{ meets } \beta' \text{ before } \beta'', \\ \beta' \text{ negatively and } \beta'' \text{ negatively then } \beta \text{ meets } \beta'' \text{ before } \beta', \\ \beta' \text{ negatively and } \beta'' \text{ positively then } \beta \text{ meets } \beta' \text{ before } \beta''. \end{cases}$$

The result follows. \square

5. SPATIAL GRAPHS

A *spatial graph* is an embedding of a finite graph in \mathbb{R}^3 , that is, the vertices are distinct points and the edges are simple curves between them in such a way that any two curves are either disjoint or meet at a common vertex. A spatial graph is called *linear* if each edge is a straight line segment. Two spatial graphs are said to be *equivalent* if they are *ambiently isotopic* [17, 21].

Theorem 3. *Let $R(G)$ and $R'(G)$ be two linear spatial representations of G . Let X and X' be the corresponding set of points in \mathbb{R}^3 associated to the vertices in such representations. If $\text{SGeom}_{\text{Aff}}(X)$ and $\text{SGeom}_{\text{Aff}}(X')$ are isomorphic then $R(G)$ is equivalent to $R'(G)$.*

Let us briefly recall the notion of spatial graphoids needed for the proof of Theorem 3.

A *graphoid* is an equivalence class of *graphoid diagrams*. A *graphoid diagram* is a graph with various distinguished degree-one vertices generically immersed in \mathbb{S}^2 , where each double point is decorated as a classical crossing labeled over/under, see Figure 24.

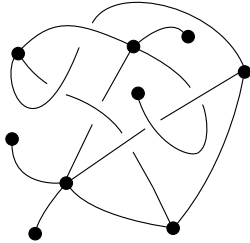
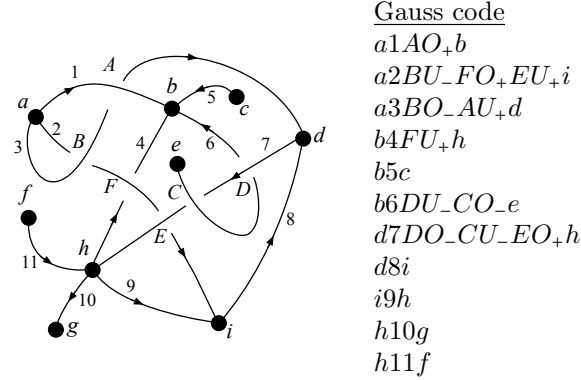


FIGURE 24. A graphoid with four distinguished degree-one vertices.

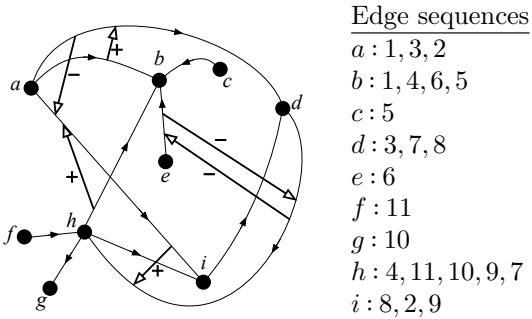
Graphoids have been studied in different contexts, for instance, in connection with a topological structure that arises in proteins [15]. A Gauss code is associated to any graphoid diagram \mathcal{G} as follows. We choose an orientation for each edge. We then write down the Gauss code for the shadow by recording whether each arrival at a crossing is an over-crossing (O) or an under-crossing (U), we can also label each crossing by its sign + or - according to handedness' rule, see Table 1. The difference with usual knots is that we add one more piece of information. For each vertex v of G , we consider the sequence of edges incident to v , appearing in counterclockwise order around v . These *edges sequences* are considered up to cyclic permutation.

TABLE 1. Gauss code of the spatial graphoid given in Figure 24.



More conveniently, Gauss codes can be understood as Gauss ‘arrow’ diagrams (as for knotoids). We also consider edges sequences around each vertex. We label points along the edges according to the crossing sequences of the Gauss code and draw an arrow between each pair of occurrences of the same label. The arrow is oriented from the undercrossing edge to the overcrossing edge and labeled with the sign of the crossing. We notice that once the arrows are drawn, the labels on the edges are redundant, and can thus be removed. In general, there is no canonical choice for ‘the immersion’ of the graph. Even if the underlying graph has a planar embedding, the order of the edges around the vertices may prevent us from using it, see Table 2.

TABLE 2. Gauss diagram of the graphoid diagram given in Figure 24.



Lemma 4. *A graphoid diagram is determined by its Gauss diagram.*

Proof. We essentially follow the same arguments as those given in the proof of Lemma 3. We only need to adapt the construction of a valid travel T in the Gauss diagram of a spatial graphoid. We have to determine the rule when T gets to a vertex of degree ≥ 3 (not existing in knotoids), that is, we have to determine the turns of the corresponding walk W when going through vertices in \mathcal{G} . For this, we use the edge sequence information, if W arrives at v along an edge e then it leaves v by following the edge f appearing before e in counterclockwise direction, that is, the next edge in clockwise direction. This new rule forces that W always turns «left» at each vertex staying in the same face, see Figure 25.

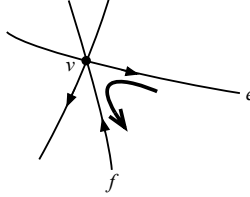


FIGURE 25. Turn of W at vertex v .

□

Remark 3. Lemma 4 can be naturally extended to virtual graphoids, that is, graphoids having virtual crossings. The virtual notion was introduced by Kauffman in his seminal paper [16]. The idea is not that a virtual crossing is just an ordinary degree-four vertex but rather that a virtual crossing is not really there (hence the name ‘virtual’).

We may now prove Theorem 3.

Proof of Theorem 3. We shall mimic the proof of Theorem 1. Let $X = (x_0, \dots, x_{n-1})$ be the tuple of points in \mathbb{R}^3 associated to the vertices (v_0, \dots, v_{n-1}) in the spatial representation of $R(G)$. Let $\pi_{x_0}(R(G))$ be the radial projection of $R(G)$ emitted from x_0 . It can be checked that such projection induces a graphoid, say \mathcal{G} , with as many distinguished vertices as the degree of the vertex corresponding to point x_0 (this can be justified in a similar way as for knotoids arising from radial projections of polygonal knots). If the diagram is not connected, then the corresponding components are unlinked, and a sequence of isotopies for each component leads to an isotopy for the whole spatial graph. Therefore, we can suppose without loss of generality that the diagram is connected. This implies that the faces of the diagram have connected boundaries and thus the arguments used in the proof of Theorem 1 work similarly in this case.

Let \mathcal{G}' be the spatial graphoid arising from $R'(G)$. We notice that any planar isotopy between the spatial graphoids \mathcal{G} and \mathcal{G}' can be extended to an isotopy between $R(G)$ and $R'(G)$ by fixing x_0 and keeping the segments $[x_0, x_i]$, for each x_i where its associated vertex v_i is a neighbor of v_0 , straight while doing the isotopy. Therefore, by Lemma 4, it is enough to show that the Gauss diagram associated to \mathcal{G} is completely determined by $\text{SGeom}_{\text{Aff}}(X) = (M_{\text{Aff}}(X), M_{\text{Wedge}}(\text{in}(X)))$ (implying that $R(G)$ can also be uniquely reconstructed from such strong geometry).

As discussed in the proof of Theorem 1, $\text{SGeom}(X)_{\text{Aff}}$ determines in the diagram : the pairs of intersecting arcs (and which one is over/under the other one) together with the corresponding sign, the local type of multiple intersection and thus their local modifications and the order of the intersections (if more than one) along a given arc. Although all of these are needed to determine \mathcal{G} , we still have to show that $\text{SGeom}(X)_{\text{Aff}}$ also determines the order of appearance, say counter clockwise, of the edges around each vertex. In fact this order is determined by $M_{\text{Aff}}(X)$ itself. Indeed, the two pieces of oriented equators $\pi_{x_0}([x_i, x_j])$, $\pi_{x_0}([x_i, x_{j'}])$ meet either positively or negatively depending on the sign of $\Delta(\pi_{x_0}(x_i), \pi_{x_0}(x_j), \pi_{x_0}(x_{j'})) = \chi(x_0, x_i, x_j, x_{j'})$. But the data of the signs of such crossings between pieces of equators is equivalent to the order at which the x_j 's appear around x_i (on the unit sphere centered on x_0). This is due to the fact that the cyclic order of the strands is given by the sign of each pair (as explained above) and, by Proposition 1, the sign of a pair $(x_i \wedge x_j), (x_i \wedge x_{j'})$ is given by the sign $\chi(x_i, x_j, x_{j'})$. Essentially, the circular order around x_i is the ‘twofold witnessed’ (first by x_0 and then by x_i) rank 2 chirotope. □

We end with the following

Question 2. Let $R(G)$ be a linear spatial representations of G . Let X be the set of points in \mathbb{R}^3 associated to the vertices of such representation. Is it true that $R(G)$ is determined by $M_{\text{Aff}}(X)$?

6. FURTHER RESEARCH DIRECTIONS

In the process of this work, a great deal on the structure, properties and extensions of the notion of strong geometry have been revealed.

6.1. Universality. Ringel's isotopy conjecture asked whether any two arrangements of lines with the same topological type can be isotoped into each other. In other words, Ringel's conjecture asked whether the realization space of rank 3 matroids is connected. The famous Mnëv's Universality Theorem [19] provides a spectacular negative solution, it states that every semi-algebraic variety is stably equivalent to the realization space of some oriented matroid, that is, the realization space of oriented matroids can have the topology of any semi-algebraic set and, in particular, it can be disconnected. As mentioned above, oriented matroids do not capture the combinatorics of the cell configuration induced by the spanned lines contrary to strong geometries that completely does. In the same flavor as for oriented matroids, an ‘inclusion-type’ generalization of the universality result à la Mnëv for rank 3 strong geometries is investigated [14].

6.2. k -equivalence. The notion of knotoid is needed to deal with the fact that the radial projection is from a point belonging to the polygonal knot. This might be avoided if given two set of points P and Q having the same strong geometry then one can show the existence of two points p and q such that $P \cup \{p\}$ and $Q \cup \{q\}$ also have the same strong geometry. In this case, we just can add this additional point from which the radial projection is applied. Figuring out the existence of these new points is not difficult when $d = 2$ but it is not straightforward for $d \geq 3$.

It turns out that the notion of strong geometry can be generalized in the planar case as follows. We consider the lines spanned by both the set of the original points and the points arising from line intersections. The latter induce a new set of lines and therefore new intersection points from which new lines can be spanned and so on. These generalizations happen to be closely related to the notion of k -equivalence between two configurations of points. A notion of ∞ -equivalence also naturally emanates. Such equivalences are recently studied in [12] in connection with some asymptotic rigidity properties. The case $k = 2$ is related to the existence of a new point to be added to a strong geometry, as discussed above.

All these investigations require further (much technical) extra work (in progress).

6.3. Adjoints. Figure 1 gives an exemple of an oriented matroid of rank 3 with two realizations that generate non-isomorphic adjoints. Moreover, there exists examples of two non-isomorphic simple oriented matroids of rank 3 that have isomorphic adjoints, see [1, 2] and [4, Exercice 5.13 (a)]. In the realizable case, Corollary 2 asserts that if the adjoints are isomorphic then the oriented matroids are equal or opposite to each other.

Acknowledgement The first author was supported by grant PRIM80-CNRS.

REFERENCES

- [1] A. Bachem, W. Kern, Adjoints of oriented matroids, *Combinatorica* **6** (1986), 299–308.
- [2] A. Bachem, W. Kern, Extension equivalences of oriented matroids, *European J. Combinatorics* **7** (1986), 193–197.
- [3] A. Bachem, A. Wanka, Matroids without adjoints, *Geometriae Dedicata* **29** (1989), 311–315.
- [4] A. Björner, M. Las Vergnas, B. Sturmfels, N. White and G. Ziegler, Oriented Matroids, *Encyclopedia of Mathematics and its Applications* **46** Cambridge University Press (1999).
- [5] G. Cairns and D.M. Elton, The planarity problem for signed Gauss words, *J. Knot Theory and Its Ramifications* **2** (1993) 359–367.
- [6] J. Chappelon, L. Martínez-Sandoval, L. Montejano, L.P. Montejano, J.L. Ramírez Alfonsín, Codimension two and three Kneser transversals, *SIAM J. Discrete Mathematics*, **32** (2018), 1351–1363.
- [7] A.L.C. Cheung, Adjoints of a geometry, *Canad. Math. Bull.* **17** (1974) 363–365.
- [8] R. Cordovil, Polarity and point extension in oriented matroids, *Linear Algebra Appl.* **90** (1987), 15–31.

- [9] R. Cordovil, Sur les matroïdes orientés de rang 3 et les arrangements de pseudodroites dans le plan projectif réel, *European J. Combinatorics* **3** (1982), 307–318.
- [10] X. Goaoc, A. Padrol, An asymptotic rigidity property of chirotope extensions, (2025), arXiv:2505.14189.
- [11] J.E. Goodman, Proof of a conjecture of Burr, Grünbaum and Sloane, *Disc. Math.* **32** (1980), 27–35.
- [12] J.E. Goodman, R. Pollack, Multidimensional sorting, *SIAM J. Computing* **12** (1983), 484–507.
- [13] J.E. Goodman, R. Pollack, Semispace of configurations, cell complexes of arrangements, *J. Comb. Th. Ser. A* **37** (1984), 257–293.
- [14] B. Gros, Strong geometry : universality of realization spaces inclusion, in preparation.
- [15] N. Gügümcü, L.H. Kauffman, P. Pongtanapaisan, Spatial graphoids, *Aequat. Math.* **98** (2024), 303–332.
- [16] L.H. Kauffman, Virtual knot theory, *Europ. J. Comb.* **20** (1999), 663–691.
- [17] L.H. Kauffman, Invariants of graphs in three-space, *Trans. Amer. Math. Soc.*, **311**(2) (1989), 697–710.
- [18] M. Las Vergnas, Personal communication (1995).
- [19] N.E. Mnëv, The universality theorem on the oriented matroid stratification of the space of real matrices, *In Discrete and Computational Geometry : Papers from the DIMACS Special Year (1990)*, J. E. Goodman, R. Pollack, and W. Steiger, Eds., vol. 6 of DIMACS Series in Discrete Mathematics and Theoretical Computer Science, DIMACS/AMS, pp. 237–244.
- [20] V. Turaev, Knotoids, *Osaka Journal of Mathematics* **49**(2) (2010), 195–223.
- [21] S. Yamada, An Invariant of spatial graphs, *J. Graph Theory*, **13**(5) (1989), 537–551.

IMAG, UNIV. MONTPELLIER, CNRS, MONTPELLIER, FRANCE

Email address: baptiste.gros@umontpellier.fr

IMAG, UNIV. MONTPELLIER, CNRS, MONTPELLIER, FRANCE

Email address: jorge.ramirez-alfonsin@umontpellier.fr